

University of Groningen

Exploring combined influences of material topography, stiffness and chemistry on cell behavior at biointerfaces

Zhou, Qihui

IMPORTANT NOTE: You are advised to consult the publisher's version (publisher's PDF) if you wish to cite from it. Please check the document version below.

Document Version

Publisher's PDF, also known as Version of record

Publication date:

2018

[Link to publication in University of Groningen/UMCG research database](#)

Citation for published version (APA):

Zhou, Q. (2018). Exploring combined influences of material topography, stiffness and chemistry on cell behavior at biointerfaces. [Groningen]: Rijksuniversiteit Groningen.

Copyright

Other than for strictly personal use, it is not permitted to download or to forward/distribute the text or part of it without the consent of the author(s) and/or copyright holder(s), unless the work is under an open content license (like Creative Commons).

Take-down policy

If you believe that this document breaches copyright please contact us providing details, and we will remove access to the work immediately and investigate your claim.

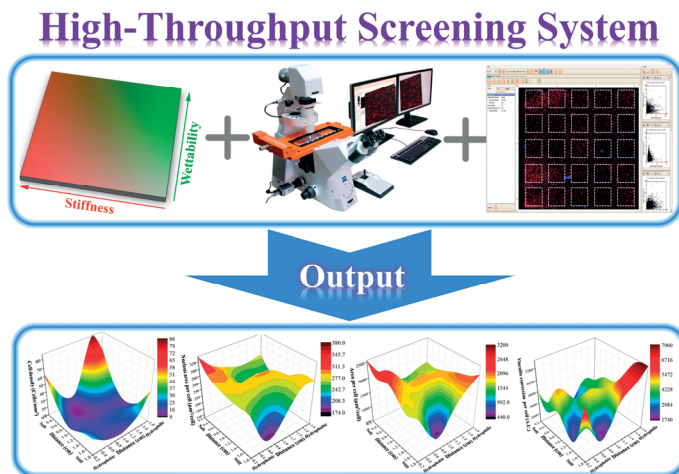
Downloaded from the University of Groningen/UMCG research database (Pure): <http://www.rug.nl/research/portal>. For technical reasons the number of authors shown on this cover page is limited to 10 maximum.

CHAPTER SIX

ORTHOGONAL DOUBLE GRADIENT FOR DETERMINING COMBINED INFLUENCES OF STIFFNESS AND WETTABILITY ON MESENCHYMAL STEM CELL BEHAVIOR

Qihui Zhou, Lu Ge, Carlos F. Guimarães, Philipp T. Kühn, Liangliang Yang, and Patrick van Rijn*

Advanced Materials Interfaces. (Accepted)



ABSTRACT

Surface gradients provide a powerful platform to accelerate multiscale design and optimization of material properties to enhance function of synthetic clinical biomaterials. Herein, a novel orthogonal double gradient is reported in which surface stiffness and wettability vary independently and continuously in perpendicular directions, providing unique combinations of stiffness and wettability over a broad range (stiffness: 6-89 MPa; water contact angle: 29-90°). It is found that mesenchymal stem cell behavior is non-linearly regulated by surface stiffness and wettability. Optimal combined material conditions are identified for promoting stem cell adhesion, spreading, nucleus size and vinculin expression, depending on both surface stiffness and wettability. This high-throughput screening system enables a more accurate understanding of the relationships between biointerface properties and biological behavior, accelerating the development of high-performance biomaterials.

6.1. INTRODUCTION

Biomaterial interfaces with the ability to direct a specific cellular response are desired in the design of optimal functioning biomedical implants and tissue engineering scaffolds, which plays an increasingly critical role in tissue engineering and regenerative medicine (TERM) [1]. It has been well-demonstrated that biomaterial parameters, such as (bio)physical cues (e.g., topography, stiffness, and wettability) and substrate-immobilized/soluble biochemical factors (composition, cytokines, extracellular matrix (ECM) proteins, and growth factors), contribute significantly to governing the behavior and function of (stem) cells both *in vitro* and *in vivo*, which offers a tremendous variability for biomaterial development [2,3]. However, most of these physicochemical properties were studied individually relying on low-throughput techniques and identifying single parameter stimulation which is not appropriate to direct cell function, since cells always interact with multiple cues simultaneously. Therefore, it is vitally important to understand and explore the combined effects of material features on the (stem) cell behavior. To efficiently study these combined effects, new technological approaches need to be developed.

As an alternative to the traditional experimental approaches using uniform substrates, surface gradient platforms offer an ideal tool to address this challenge *in vitro* and *in vivo* [4–6], enabling elucidation of cell-material interactions in a high-throughput screening (HTS) strategy. Numerous research groups developed diverse gradient surfaces with different material features (e.g., topography, stiffness, wettability, or biochemistry) to successfully identify material-cell responses (such as adhesion, spreading, proliferation and differentiation) [4,7–9] and study cell directed migration (e.g., topotaxis [7], chemotaxis [10], and durotaxis [11]). However, it remains a huge bottleneck to simultaneously and independently pattern multiple parameters at once on a single substrate. Particularly, combining chemical patterning and mechanical properties over a broad range, reflecting clinically relevant biomaterials, is more challenging as these two are very closely related, because alterations in stiffness are often induced by a change in chemistry (cross-linking). Design and application of such combinatorial platform systems would serve as exceptional starting points to capture multiple material properties in an enhanced HTS manner and be able to direct cell responses.

In this work, we focused on material surface stiffness and wettability of a synthetic clinically used material, because both parameters offer critical cues to direct (stem) cell behavior and not always in a predictive fashion [4,8,12,13]. It is pertinent to identify optimal surface characteristics for directing cellular response and the design of biomedical devices applied in TERM. Moreover, they have different interaction modes with (stem) cells. Wettability influences mostly the adsorbing proteins to which the cell responds [14,15], whereas stiffness works as a crucial indirect cue that strongly affects cell behavior and function through mechanosensing and mechanotransduction processes [16,17]. Herein, we created an orthogonal double gradient based on PDMS of which stiffness and wettability can be manipulated with air plasma oxidation. It enabled us to pattern gradients of different substrate properties in a perpendicular direction providing every location on the surface with unique parameter combinations. Surface stiffness and wettability were systematically assessed by atomic force microscopy and water contact angle, respectively. This multivariate orthogonal platform was utilized to probe the behavior of human bone marrow-derived mesenchymal stem cells (hBM-MSCs) in a HTS approach. It enabled the elucidation of their interaction with combined material parameters as well as identifying

the extremities in cell response towards these combined parameters, which provides both fundamental insights as well as the translation of properties towards a clinical material often used for implants and medical device coatings namely, silicone rubber.

6.2. RESULTS AND DISCUSSION

A particular aim was to consider a simple and cheap fabrication process with a commonly used biomaterial and thereby not only provide fundamental insights in cell behavior at complex biointerfaces but also to have a potential clinical translation factor. PDMS was selected because of its cost-efficiency, non-toxic, inert, easy to process properties and its ubiquity as an implantable biomaterial and tissue engineering scaffold [18,19]. The fabrication process of orthogonal double gradients based on PDMS is illustrated in **Figure 1**. We controlled PDMS stiffness and wettability independently and in a spatially controlled fashion via plasma oxidation and chemical modification. Firstly, the unidirectional double gradient with stiffness and wettability was generated by exposing the PDMS surface to air plasma with a 2×2 cm-30° mask covering the gradient area. Plasma oxidation (60 seconds, 30 mtorr) causes the PDMS surface to become stiffer and more hydrophilic, increasing both parameters from the closed to the open side of the mask. Subsequently, the plasma generated gradient was chemically modified overnight by immersion in a solution of ethanol, ammonia hydroxide (30%) and trimethoxypropylsilane, which results in a hydrophobic monolayer thereby removing the wettability gradient while maintaining the stiffness gradient. Lastly, we placed a 2×2 cm-30° mask with a 90° orientation relative to the stiffness gradient on the same area and performed an air plasma treatment under mild conditions (20 seconds, 500 mtorr). A wettability gradient orthogonal to the stiffness gradient was generated by modifying the monolayer alone therefore not affecting the stiffness gradient (**Figure 2A-D**). In addition, unidirectional single parameter gradients (stiffness and wettability) and unidirectional double gradient were prepared as controls and to illustrate the strength of the orthogonal double gradient. It is important to validate the results in comparison to unidirectional single or unidirectional double gradient surfaces, because our work and other previous studies have exemplified single gradient surfaces as an accurate HTS tool to assess (stem) cell behavior and function [20,21]. This generation approach is simple, cost-efficient, highly reproducible, and does not require sophisticated instrumentation such as clean room facilities or complex conjugation chemistry. Moreover, the formed platform is compatible with general *in vitro* cell culture approaches, such as routine commercial slides, and standardized square and round Petri dishes.

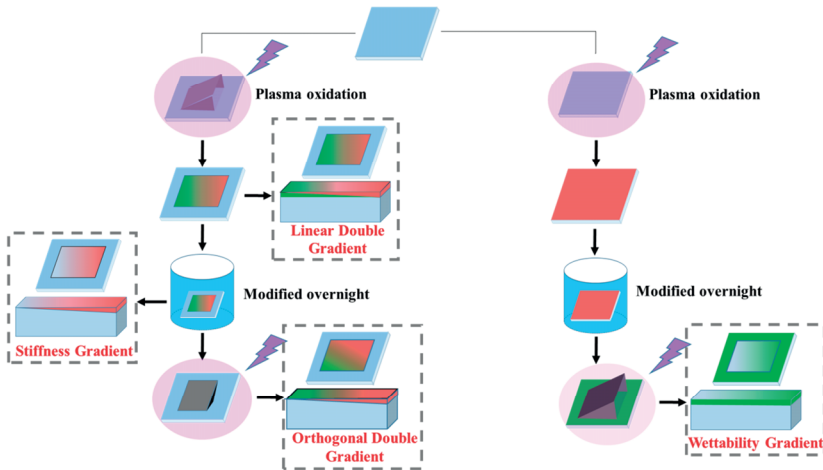


Figure 1. Formation of unidirectional single and orthogonal double surface gradients. Gradients are prepared by sequential air plasma oxidation treatments and chemical modification using silanization reactions. Choosing various specific combinations in either unidirectional gradients of either wettability or stiffness, unidirectional double gradient, and the desired orthogonal double gradient.

Surface stiffness and wettability were measured by the surface Young's modulus using atomic force microscopy (AFM) and water contact angle (WCA) in five positions spaced around 5.0 mm apart along the gradients, respectively. For the orthogonal double gradient, **Figure 2A-D** display that stiffness increased from 6 MPa to 89 MPa on the x-axis while WCA decreased from 90° to 29° on the y-axis. Importantly, we evaluated the stiffness and wettability on PDMS substrate in the direction perpendicular to the direction of the gradient of interest on the double patterned surface. There was no difference in stiffness in the direction of the wettability gradient. Additionally, the wettability was not affected in the direction of the stiffness gradient. The unidirectional stiffness gradient obtained ranges from 6 MPa to 91 MPa with around 90° WCA. Its stiffness range is similar to the orthogonal double gradient. The unidirectional wettability gradient decreased very steadily in WCA from 86° to 33° with uniform stiffness. For unidirectional double gradient, the wettability ranges from a WCA of 93° to 23°. The stiffness increased from 7 MPa to 90 MPa. These results demonstrated that the surface stiffness and wettability can be tailored by plasma oxidation depending on the chosen oxidation parameter. Applying air plasma oxidation under the used conditions does not affect the surface structure (topography) as was demonstrated in our previous work [3].

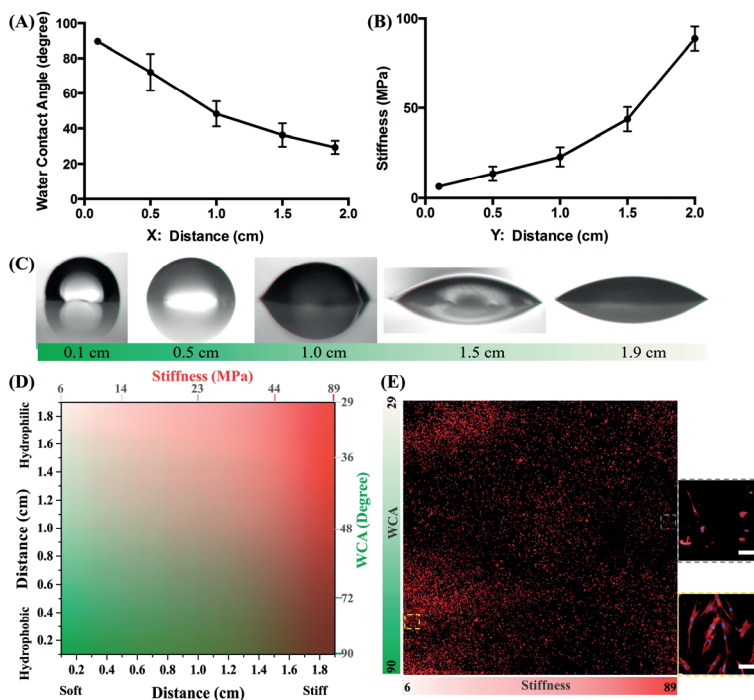


Figure 2. (A, B) Dependence of the water contact angle and stiffness on the distance within the orthogonal double gradient. (C) Water contact angle images with different positions along the orthogonal double gradient surface. (D) The heat map of the orthogonal stiffness and wettability gradient drawn using the above figure A and B by the Origin9 software. (E) hBM-MSCs cultured on the orthogonal double gradient for 24 hours. hBM-MSCs are stained using phalloidin for F-actin (red) and DAPI for nucleus (blue). Scale bar: 100 μ m.

To demonstrate the power of our HTS technology and whether the continuous variation of surface properties could elicit a cell response, we cultured hBM-MSCs on the developed gradient platforms for 24 h, imaged the cells via automated fluorescence microscopy, and quantified the cell response on 25 areas (division of the surface in a 5 \times 5 grid). Here, hBM-MSCs were employed as a model cell type, which has previously shown to depend strongly on surface stiffness and wettability [2-4].

Cell behavior was observed by automated fluorescence microscopy (TissueFAXS) in a high-throughput manner, which enabled the observation of the surfaces as a whole. As depicted in **Figure 2E**, we can directly observe hBM-MSC distribution across the whole surface of the 2 \times 2 cm orthogonal double gradient with the capability of zooming in even until a single cell level (**Figure 2E inset**). The overview image of the orthogonal double gradient displays higher cell surface coverage in WCA ranging from 29 $^{\circ}$ -36 $^{\circ}$ and 48 $^{\circ}$ -90 $^{\circ}$ on the soft part (6-19 MPa) of the substrate. However, there is similar cell surface

coverage on the stiffer range from 19 to 89 MPa in WCA range from 29° to 90°. The results indicate that cell surface coverage was affected synergistically by surface stiffness and wettability. In addition, on the single stiffness gradient surface, cell surface coverage decreased with the increasing of surface stiffness (**Figure S1B**). On the single wettability gradient surface, cell surface coverage increased with the decreasing WCA (**Figure S1C**). On the unidirectional double gradient surface, cell surface coverage first decreased and then increased with the simultaneous increasing of surface stiffness and wettability (**Figure S1D**). The unidirectional stiffness gradient, wettability gradient, and double gradient, provided similar results compared to the specific positions on the orthogonal double gradient surface indicated by the differently colored lines (**Figure S1**). This similarity indicates that the HTS platform of orthogonal double gradient surface is a simple, efficient and accurate strategy to elicit cell-surface interactions over a broad range identifying parameter synergy (**Figure S2**).

For a better understanding of cell behavior on gradients without focusing on a specific biological question, cell number, area/cell, nucleus area and vinculin expression were determined by quantitative analysis of the positively stained cells using the high-throughput analysis technique (TissueQuest software). To determine how pairwise combinations of stiffness and wettability regulate cell behavior, we measured the cells at 25 (5×5 grid) uniformly-spaced locations across the whole orthogonal double gradient surface (2×2 cm). At least 250 cells were analyzed on each position. 3D heat map representations show the cell density, nucleus area, area/cell, and vinculin expression across the total gradient surface after 24 hours culture (**Figure 3A-D**). On the orthogonal double gradient possible areas of interest are easily observed as the plot indicates whether the surface parameters elicit either high or lower biological responses.

Figure 3A displays that the cell density increases with increasing the surface wettability and decreasing the stiffness. It indicates that both inputs are cooperative, as the highest cell density was observed on substrate WCA (35-39°) and stiffness (8.2-9.3 MPa). This output offers the significant information for accelerating tissue repair and regeneration. Identifying optimum properties for tissue repair and regeneration remains a great challenge for polymer or inorganic materials due to lack of surface cell recognition sites. Studies by other groups reported that higher initial rate of cell attachment and cell density were found on more hydrophilic surfaces [22,23]. In contrast, others found that cells attached and proliferated faster on more hydrophobic substrates with WCA from 55-70° [8,21]. These different or even contradictory results were likely due to the various material chemistry, surface topographies and stiffness employed or the narrow ranges of surface wettability used. It is challenging to strictly control the material surface that can be defined with comparable features. Although, these studies demonstrate the potential of surface wettability for controlling cell behavior, it is important to note that most of them investigated cell phenomena on substrates with uniform mechanical properties in low efficiency. Herein, our gradient platform offers an ideal approach to systematically evaluate the influence of surface wettability and stiffness in a dependent fashion on cell behavior relying on a single material (PDMS). This platform system condenses experiment quantities vastly for which generally numerous substrates of discrete stiffness and wettability would be needed. Compared to cell behavior on the unidirectional single and double gradients, the cell numbers were comparable and there is a similar trend with the specific positions on the orthogonal double gradient surface (**Figure S2**). The similarity

validates the HTS substrate developed here. Importantly, if only the unidirectional gradients would be employed, interesting cell responses would have remained unidentified. The nucleus size is closely related to nuclear functional activity and subsequently cell differentiation [24]. To better understand the relationship between surface properties and nucleus size, a map of nucleus area per cell was generated (**Figure 3B**). We directly find the largest nucleus area per cell on the orthogonal double gradient with stiffness 6-13 MPa and wettability 75-90°. Cells located on the soft side displayed a decrease in the nucleus area per cell with increasing wettability going from an average nucleus area of $333\pm 28 \mu\text{m}^2$ at the hydrophobic side to $245\pm 14 \mu\text{m}^2$ at the hydrophilic end. In contrast, when cells were on the stiff side, the nucleus area per cell increases with the increasing wettability from a nucleus area of $185\pm 42 \mu\text{m}^2$ at the hydrophobic portion to an average nucleus area of $282\pm 13 \mu\text{m}^2$ at the hydrophilic end. These results indicate that nucleus area was mediated cooperatively by surface stiffness and wettability. Within the same analysis, the cell spreading is visualized by analyzing via phalloidin stained actin. **Figure 3C** shows that cells on the hydrophilic side increase their spreading area with increasing stiffness from an average cell area of $1732\pm 44 \mu\text{m}^2$ at the soft side to $2290\pm 218 \mu\text{m}^2$ at the stiff end. In contrast, when cells were on the hydrophobic side, area per cell decreases with increasing stiffness from an average cell area of $2556\pm 168 \mu\text{m}^2$ at the soft side to $1735\pm 194 \mu\text{m}^2$ at the stiff end. The largest area per cell is found on the position with stiffness (8-50 MPa) and wettability (79-85°). Clearly, cell area is regulated cooperatively by surface stiffness and wettability. In addition, we observed the positive correlation between nucleus area and actin cytoskeleton area. Most studies reported that cells adhered on stiffer bulk substrates displayed increased cytoskeletal development and more extensive spreading [25,26]. In contrast, recent studies of Baker and Jing indicated that cellular contractile forces could recruit nearby fibers with lower stiffness, which leads to increasing ligand density around the cell and enhancing the formation of β -integrin, vinculin and focal adhesions and inducing stem cell spreading [27,28]. Although these studies have provided many new insights, it is important to note that most of the earlier studies investigated cell behavior on samples with uniform mechanical properties. There is a need for cross-combination studies to obtain a deeper insight into such behavior, since a surface will always be a combination of properties, e.g., stiffness, topography, and wettability. Vinculin as an integral protein is used as a critical factor in cellular interaction with biomaterial substrates, which mediates transmission of signals between the cell-matrix and cell-cell junctions, promotes focal adhesion formation as a driving force, and connects the focal adhesion with the actin cytoskeleton [29,30]. We measured vinculin expression using a quantitative analysis of fluorescence intensity by TissueQuest software. hBM-MSCs showed significant variation in vinculin expression as a function of substrate stiffness and wettability (**Figure 3D**). At the hydrophilic side, we observed an increase in vinculin expression per cell with increasing substrate stiffness. In particular, we found substantial regulation of vinculin expression at the highest stiffness in the hydrophilic section. Our results reveal that vinculin is differently mechanosensitive when specific surface parameter combinations are applied and that the material features modulate vinculin regulation in a complex and nonlinear fashion. We identified the material features for maximum vinculin expression (stiffness: 40-89 MPa, WCA: 29-34°) using the orthogonal double gradient.

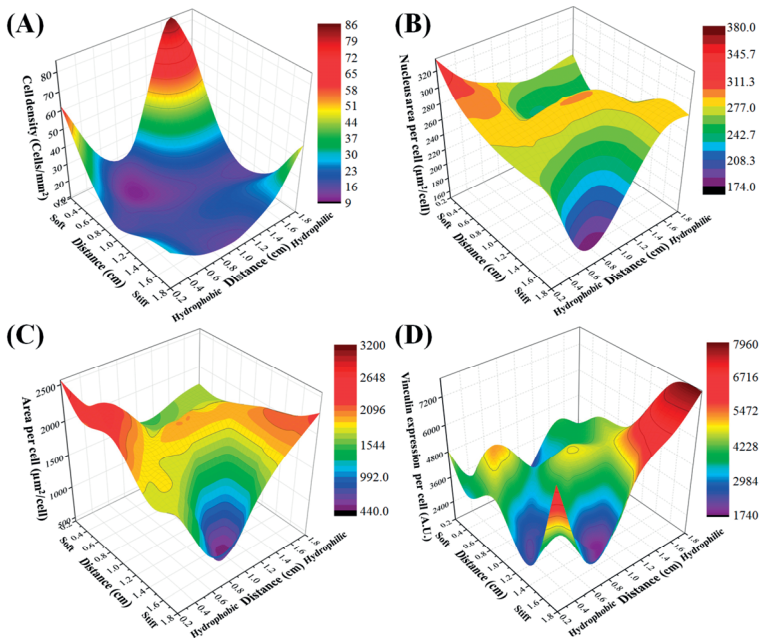


Figure 3. hBM-MSC behaviors on the orthogonal double gradient. (A) cell density, (B) nucleus area per cell, (C) area per cell, (D) vinculin expression per cell after 24 h culture ($n = 3$).

The orthogonal double gradient platform developed herein provides a powerful strategy to analyze numerous combinations of two surface parameters influencing cell interactions with biomaterials. In addition, stem cell responses on the platform were characterized by automated fluorescence microscope (TissueFAXS) in a high-throughput fashion, which enabled the observation of the surfaces as a whole. Cell behavior was determined by a quantitative analysis of the positively stained cells using the high-throughput analysis technique (TissueQuest software). Future endeavors will also include the automated processing of results to complement the HTS approach as data processing become the limiting factor. The combination of a novel HTS platform, advanced imaging, and efficient analysis technologies is used to accelerate the creation of next generation biomaterials for biomedical engineering. Expectantly, the big data obtained from HTS, named “materiobiology [1] genome”, could be utilized as inputs into computer models to simulate and output the accurate prediction of biomaterial parameters as a function of cell response.

6.3. CONCLUSION

In summary, we developed a novel approach to elucidate combined physical parameter influences on cellular behavior based on the orthogonal double gradient surface and thereby gain insights in desired hBM-MSC responses. We found that most cell responses are nonlinearly regulated by material stiffness and wettability. The optimal combined surface properties for promoting hBM-MSCs adhesion, nucleus size, spreading as well as vinculin expression were identified based on the orthogonal double gradient platform. The strategy presented allows for efficient analysis of multiple cue-response relationships to develop biomaterial libraries, which could accelerate the development of desired biomedical implants and tissue engineering scaffolds.

6.4. EXPERIMENTAL SECTION

PDMS film preparation. Polydimethylsiloxane (PDMS) films were prepared from a commercial elastomer kit based on the supplier's information (Dow Corning). The prepolymer and cross-linker were mixed at a 10:1 ratio by weight. The 30 g mixture was vigorously stirred with a spatula and then was degassed for 15 min under vacuum to remove the air bubbles completely, and poured on 12×12 cm cleaned petri dishes ensuring an equal thickness. The PDMS was then cured at 70 °C overnight to ensure complete crosslinking.

Generation of planar wettability and stiffness gradients. Unidirectional double gradient: The PDMS substrate was exposed to air plasma for 1 minute at 30 mtorr with a 2cm-30° mask covering the gradient area. Plasma oxidation causes the PDMS surface to become stiffer and more hydrophilic, increasing both parameters from the close side to open side of the mask. This results in a unidirectional double (both vary in the same direction) gradient of wettability and stiffness. The gradient substrate was stored in buffer and used the same day for cell experiments to prevent hydrophobic recovery.

Single stiffness gradient: In order to isolate the stiffness gradient from the obtained unidirectional double gradient, it was modified overnight in a liquid solution of 30 mL absolute ethanol, 2.4 mL ammonia hydroxide (30%) and 80 μL trimethoxypropylsilane. The samples were then rinsed with absolute ethanol to remove any remaining contaminants. This modification results in a hydrophobic monolayer thereby removing the wettability gradient while keeping the stiffness gradient intact.

Single wettability gradient: To generate a single wettability gradient, unmodified PDMS surfaces were oxidized in plasma for 10 minutes at 200 mtorr, generating a stiff and active surface to then be liquid modified as described in single stiffness gradient preparation. The wettability gradient was created by using a 2cm-30° mask and placing the sample in 500 mtorr plasma oxidation for 20 seconds. This short and high-pressure oxidation allows for monolayer modification and wettability gradient generation without altering the stiffness

on the PDMS substrate. The gradient substrate was stored in buffer and used the same day for cell experiments to prevent hydrophobic recovery.

Orthogonal double gradient: Orthogonal double wettability and stiffness gradients were obtained by using unidirectional stiffness gradients as described above with the homogenous hydrophobic surface and then placing a 2cm-30° mask with a 90° orientation in relation to the stiffness gradient and placing the sample in the plasma oven for 20 seconds with a pressure of 500 mtorr. After that, a wettability gradient orthogonal to the stiffness gradient was generated by modifying the monolayer alone therefore not affecting the stiffness gradient. The gradient was stored in buffer and used the same day for cell experiments to prevent hydrophobic recovery.

Characterization of PDMS gradient surfaces. The surface stiffness was assessed by the surface Young's modulus using the AFM device with nanoscope V as the software. All AFM data was obtained using Bruker Cantilevers made from silicon nitride with silicon tips. The wettability of the samples was measured using a custom-built tensiometer, using droplets of milliQ water in a sessile drop method. The water contact angle value and droplet pictures were obtained using a specifically coded Matlab program. Wettability was determined directly after sample preparation.

Cell culture. Human bone marrow-derived mesenchymal stem cells (hBM-MSCs, Lonza™) were cultured in the growth medium consisted of Alpha modified Eagle medium (Gibco), 10% (v/v) fetal bovine serum (Gibco) and 0.1% (v/v) ascorbic acid 2-phosphate (Sigma). Cells were incubated at 37°C, 5% CO₂. The cells were harvested at approximately 80-90% confluency from T75 culture flasks by trypsin for ~5 min at 37°C for further subcultures.

Cell adhesion studies. All samples (2.0×2.0 cm) were treated with 70% ethanol for sterilization and placed in 6-well plates and then washed with PBS before use. Afterwards, hBM-MSCs were seeded onto the samples in 6-well plates at a density of 3×10^4 cells/well and allowed to grow for 24 h. The hBM-MSCs were fixed with 3.7% paraformaldehyde (Sigma-Aldrich) in PBS for 20 min at room temperature, and subsequently washed three times with 1 mL PBS. Afterward, the cell membrane was permeabilized with 0.5% TritonX-100 (Sigma-Aldrich) solution for 3 min. A 5% BSA in PBS solution was added for 30 min to block non-specific binding. After withdrawing the BSA solution, the primary antibody against vinculin (clone hVin-1, Sigma, 1:100) was used in combination with a secondary FITC-labeled goat-anti-mouse antibody (Jackson Immunolab, 1:100). In addition, TRITC-phalloidin and DAPI were used to stain the cell cytoskeletal filamentous actin and nucleus, respectively. The samples were automatically scanned with Zeiss AxioImager.Z1 fluorescence inverted microscope at 10× magnification controlled by TissueFAXS software (TissueGnostics GmbH, Vienna, Austria). Images were acquired at the same acquisition parameters (exposure time, gain and threshold setting) and combined together using the Tissue-Gnostics software. The cell results (i.e., cell density, nucleus area per cell, area per cell and vinculin expression per cell) were quantified using TissueQuest™ software (TissueGnostics GmbH, Vienna, Austria). And, the area and intensity of fluorescence were normalized to number of cells analyzed using the DAPI channel. Details of the method have been described previously^[31,32].

ACKNOWLEDGEMENTS

Q.H.Z., L.G., and L.L.Y. are very grateful for financial support of the China Scholarship Council (No. 201406630003; 201707720058; 201608310113). Part of the work has been performed in the UMCG Microscopy and Imaging Center (UMIC), sponsored by NWO-grant 40-00506-98-9021. Joop de Vries is gratefully acknowledged for help with AFM and plasma system maintenance. Klaas Sjollema is kindly acknowledged for help with TissueFAXS microscope.

SUPPORTING INFORMATION

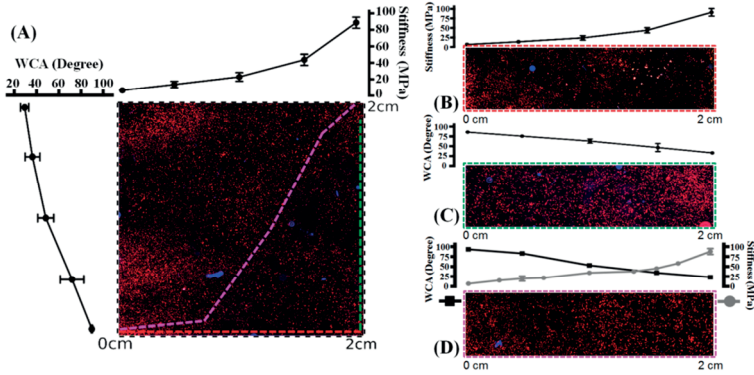


Figure S1. hBM-MSCs cultured on the orthogonal double gradient (A), single stiffness gradient (B), single wettability gradient (C), and unidirectional double gradient (D) for 24 hours. hBM-MSCs are stained using phalloidin for F-actin and DAPI for the nucleus. The nuclei are not observed at these magnifications. The same dashed color lines (red, green, and pink) between figure S1A and S1B-D indicate the similar stiffness and wettability, respectively.

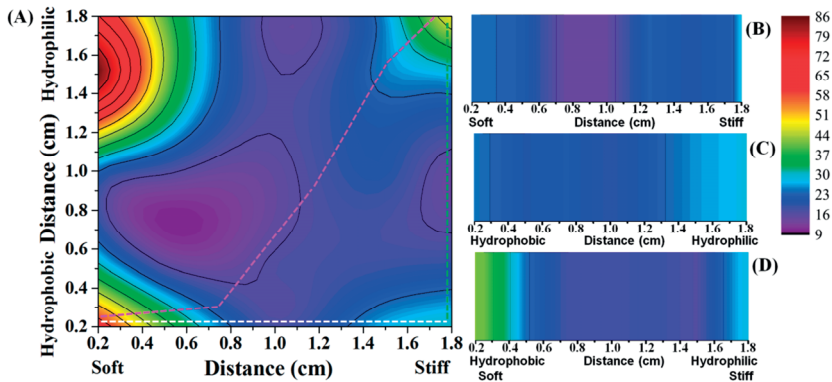


Figure S2. hBM-MSC density on the orthogonal double gradient (A), single stiffness gradient (B), single wettability gradient (C), and unidirectional double gradient (D) after 24 h culture. The stiffness and wettability on the dashed line of white, green, and pink within the orthogonal double gradient have the similar value to the unidirectional stiffness gradient, wettability gradient, and double gradient, respectively. The same dashed color lines (white, green, and pink) between figure S2A and S2B-D indicate the similar stiffness and wettability, respectively.

REFERENCES

- [1] Y. Li, Y. Xiao, C. Liu, *Chem. Rev.* **2017**, *117*, 4376.
- [2] A. M. Schaap-Oziemlak, P. T. Kühn, T. G. van Kooten, P. van Rijn, *RSC Adv.* **2014**, *4*, 53307.
- [3] Q. Zhou, O. Castañeda Ocampo, C. Guimarães, P. Kuhn, T. van Kooten, P. van Rijn, *ACS Appl. Mater. Interfaces* **2017**, *9*, 31433.
- [4] P. T. Kühn, Q. Zhou, T. A. B. van der Boon, A. M. Schaap-Oziemlak, T. G. van Kooten, P. van Rijn, *ChemNanoMat* **2016**, *2*, 407.
- [5] F. Hulshof, B. Papenburg, A. Vasilevich, M. Hulsman, Y. Zhao, M. Levers, N. Fekete, M. de Boer, H. Yuan, S. Singh, *Biomaterials* **2017**, *137*, 49.
- [6] A. L. Hook, D. G. Anderson, R. Langer, P. Williams, M. C. Davies, M. R. Alexander, *Biomaterials* **2010**, *31*, 187.
- [7] J. Park, D.-H. Kim, H.-N. Kim, C. J. Wang, M. K. Kwak, E. Hur, K.-Y. Suh, S. S. An, A. Levchenko, *Nat. Mater.* **2016**, *15*, 792.
- [8] J. Lee, G. Khang, J. Lee, H. Lee, *J. Colloid Interface Sci.* **1998**, *205*, 323.
- [9] A. D. Rape, M. Zibinsky, N. Murthy, S. Kumar, *Nat. Commun.* **2015**, *6*, 8129.
- [10] P. Devreotes, C. Janetopoulos, *J. Biol. Chem.* **2003**, *278*, 20445.
- [11] C.-M. Lo, H.-B. Wang, M. Dembo, Y. Wang, *Biophys. J.* **2000**, *79*, 144.
- [12] D. E. Discher, P. Janmey, Y.-L. Wang, *Science* **2005**, *310*, 1139.
- [13] L. Hao, H. Yang, C. Du, X. Fu, N. Zhao, S. Xu, F. Cui, C. Mao, Y. Wang, *J. Mater. Chem. B* **2014**, *2*, 4794.
- [14] Y. Mei, K. Saha, S. R. Bogatyrev, J. Yang, A. L. Hook, Z. I. Kalcioğlu, S.-W. Cho, M. Mitalipova, N. Pyzocha, F. Rojas, K. J. Van Vliet, M. C. Davies, M. R. Alexander, R. Langer, R. Jaenisch, D. G. Anderson, *Nat. Mater.* **2010**, *9*, 768.
- [15] Y. Tamada, Y. Ikada, *J. Colloid Interface Sci.* **1993**, *155*, 334.
- [16] W. J. Hadden, J. L. Young, A. W. Holle, M. L. McFetridge, D. Y. Kim, P. Wijesinghe, H. Taylor-Weiner, J. H. Wen, A. R. Lee, K. Bieback, *Proc. Natl. Acad. Sci.* **2017**, *114*, 5647.
- [17] V. Vogel, M. Sheetz, *Nat. Rev. Mol. Cell Biol.* **2006**, *7*, 265.
- [18] A. J. T. Teo, A. Mishra, I. Park, Y.-J. Kim, W.-T. Park, Y.-J. Yoon, *ACS Biomater. Sci. Eng.* **2016**, *2*, 454.
- [19] E. Pedraza, A.-C. Brady, C. A. Praker, C. L. Stabler, *J. Biomater. Sci. Polym. Ed.* **2013**, *24*, 1041.
- [20] Q. Zhou, P. T. Kuhn, T. Huisman, E. Nieboer, C. van Zwol, T. G. van Kooten, P. van Rijn, *Sci. Rep.* **2015**, *5*, 16240.
- [21] M. Zelzer, R. Majani, J. W. Bradley, F. R. A. J. Rose, M. C. Davies, M. R. Alexander, *Biomaterials* **2008**, *29*, 172.
- [22] F. Grinnell, M. K. Feld, *J. Biol. Chem.* **1982**, *257*, 4888.
- [23] J. Wei, T. Igarashi, N. Okumori, T. Igarashi, T. Maetani, B. Liu, M. Yoshinari, *Biomed. Mater.* **2009**, *4*, 45002.
- [24] X. Liu, R. Liu, B. Cao, K. Ye, S. Li, Y. Gu, Z. Pan, J. Ding, *Biomaterials* **2016**, *111*, 27.
- [25] A. S. Rowlands, P. A. George, J. J. Cooper-White, *Am. J. Physiol. Physiol.* **2008**, *295*, C1037.
- [26] A. J. Engler, S. Sen, H. L. Sweeney, D. E. Discher, *Cell* **2006**, *126*, 677.
- [27] B. M. Baker, B. Trappmann, W. Y. Wang, M. S. Sakar, I. L. Kim, V. B. Shenoy, J. A. Burdick, C. S. Chen, *Nat. Mater.* **2015**, *14*, 1262.
- [28] J. Xie, M. Bao, S. M. C. Bruekers, W. T. S. Huck, *ACS Appl. Mater. Interfaces* **2017**, *9*, 19630.
- [29] C. Grashoff, B. D. Hoffman, M. D. Brenner, R. Zhou, M. Parsons, M. T. Yang, M. A. McLean, S. G. Sligar, C. S. Chen, T. Ha, *Nature* **2010**, *466*, 263.
- [30] J. D. Humphries, P. Wang, C. Streuli, B. Geiger, M. J. Humphries, C. Ballestrem, *J. Cell Biol.* **2007**, *179*, 1043.
- [31] C.-C. Wu, C.-C. Lien, W.-H. Hou, P.-M. Chiang, K.-J. Tsai, *Sci. Rep.* **2016**, *6*, 27358.
- [32] M. Uta, L. E. Sima, P. Hoffmann, V. Dinca, N. Branza-Nichita, *Biomed. Microdevices* **2017**, *19*, 3.

